THREE EXPERIMENTAL APPLICATIONS OF HEALTH ALGORITHMS TO IMPROVE INFRASTRUCTURE INSPECTION

Elizabeth K. Ervin

The University of Mississippi, Carrier Hall 202, Box 1848, University, MS 38677, USA

eke@olemiss.edu

ABSTRACT

This paper presents three applications of structural health evaluation from data collection to damage location. The first test setup was a standard railway track with an adjustable sleeper to allow for artificial defects. The second test setup was a student-built reinforced concrete bridge with various rubber bearings to represent joint softening. The third test location was a skewed on-campus highway bridge built in 1940 with no maintenance record. The obtained data sets were analyzed with an in-house structural health evaluation program, performing modal decomposition and applying twelve different damage detection algorithms.

KEYWORDS : *evaluation, infrastructure, inspection, maintenance, civil engineering.*

INTRODUCTION

Causing loss of use and sometimes life, bridge collapses are always high profile and hit many wallets. The economic benefits of condition-based maintenance are well established, including reduced visual inspection and potentially longer structural life. More accurate estimation of remaining life could potentially prevent collapse but, at a minimum, will aid decision-making on a bridge's upkeep.

Results are presented herein for three experimental efforts: a railroad, a scaled reinforced concrete bridge, and an operational on-campus bridge. Traditional cabled accelerometer sensing as well as a Laser Doppler vibrometer (LDV) were used as infrastructure inspection tools. Real-time health evaluation and condition-based maintenance are the ultimate aspirations, and a potential product could be a mobile inspection vehicle that would ride along any bridge.

Each experiment was analyzed using the Structural Health Evaluation (SHE) program developed in the Multi-Function Dynamics Laboratory (MFDL) at the University of Mississippi. The program consists of four major modules: 1) input, 2) modal decomposition, 3) health algorithms, and 4) output. Time history input from any sensor is prescribed as any comma-separated text file. The degrees of freedom and their locations must be recorded universally as well. For complete adaptability, the team built one integrated program that provides mode shapes for user-selected peaks. The user then correlates two modes (baseline vs. damaged) upon which numerous structural health algorithms are applied. Visual output was completed for user ease: color-coded output is displayed to the screen: note that the thresholds are arbitrarily selected at this time.

1 RAILROAD

As shown in Figure 1a, an on-campus mock railway track was constructed to code for a medium heavy commuter rail. Including ties, plates, screws, clips, and rail, components for a five-span monorail were donated Atlantic Track and Turnout in Memphis, TN. In order to physically model the damage mechanism of tie settlement, five stainless steel sheets were placed under the center tie.

The measurement capabilities of the LDV, Model Polytec PDV100, were examined, and the LDV must be mechanically decoupled from the ground in order to measure the low frequency vibration of the rail track structure. As light moving platforms caused too much interference, the

LDV and its linear stage were mounted on a massive forklift platform (Figure 1b). The linear stage had a motor that could continuously move the LDV along the rail at a speed of 20 mm/s.
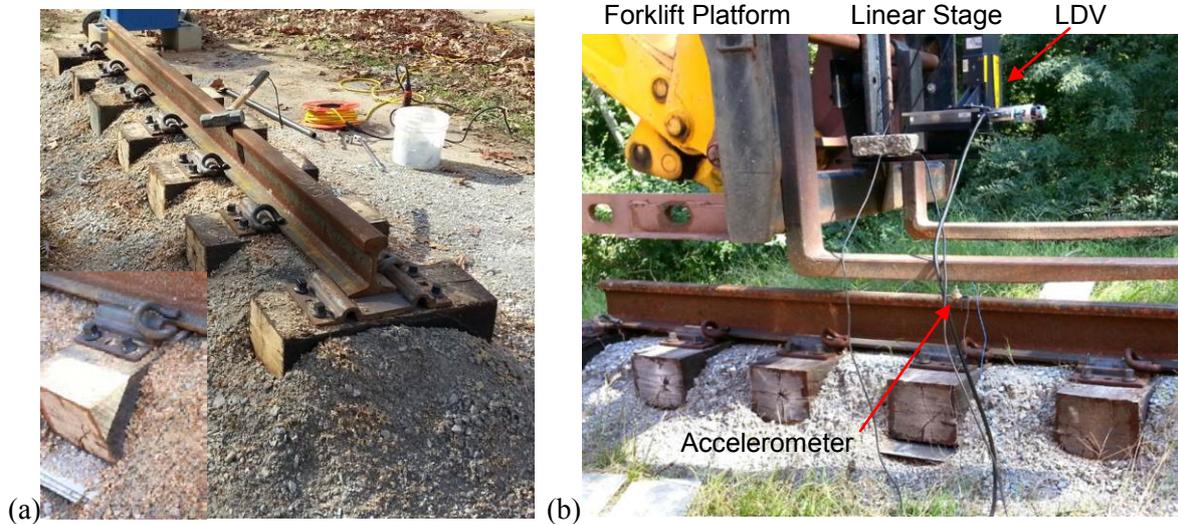

(a)   (b)

Figure 1: Rail setup and instrumentation

Vibration of the monorail structure was excited using an impact on the rail at a point located approximately ten centimeters from the right end of the rail. The resulting vibration over the center tie was measured with a LDV and an accelerometer simultaneously. Each optical measurement was completed in parallel with the accelerometer measurement for verification. Note that retroreflective tape on the rail surface enhanced reflectivity.

Structural defects were induced at the center tie, and measurements occurred in the two nearby spans. Vibration response was measured with the LDV in two modes: stationary and moving. These results were compared to the undamaged baseline, or "as-built" configuration. The LDV only identified variations near 400 Hz and 800 Hz. Qualitatively, the induced defect of one loose tie-plate screw represented minimal damage, as just one of four screws is altered that attaches the tie plate to the tie. With two loose tie-plate screws, both 400 Hz and 800 Hz peaks split. Four loose tie-plate screws represented the maximum release in the connection between the plate and the tie. This defect causes major changes in the LDV vibration spectra: significant magnitude increase of the peak near 400 Hz and lesser response near 800 Hz. With all loose screws and a cracked tie plate, this trend continued.

In order to quantitatively compare the data, the developed structural health program was applied. The case of four loose screws was examined for a common frequency range of structural interest, 0 Hz to 250 Hz. Eight and nine modes were identified for the baseline and the damaged cases, respectively. Differentiation between the modes with the naked eye was difficult; however, Mode 2 was a rigid body mode, and Mode 3 involved center tie deflection. Modes were coordinated by inspection of mode shape similarities: this is a subjective and qualitative process. As an example, Mode 4 is shown in Figure 2a. Note that natural frequencies generally decreased with damage, but there was no significant change to Mode 3's natural frequency.

Modal Assurance Criterion (MAC) showed that Mode 3 was 97% damaged. These results mean that the four loose screws decoupled the tie from the rail and allowed it to vertically "rattle." Mode 1 also showed 92% damage, which means that torsion of the center tie also occurred. Six damage location algorithms were also applied, and most indicators show significant damage at the center tie and most commonly on the right side of the tie, as in Figure 2b by Coordinated Modal Assurance Criterion (COMAC). Note that the color-coded thresholds are arbitrary and will require more research to set for any given setup.
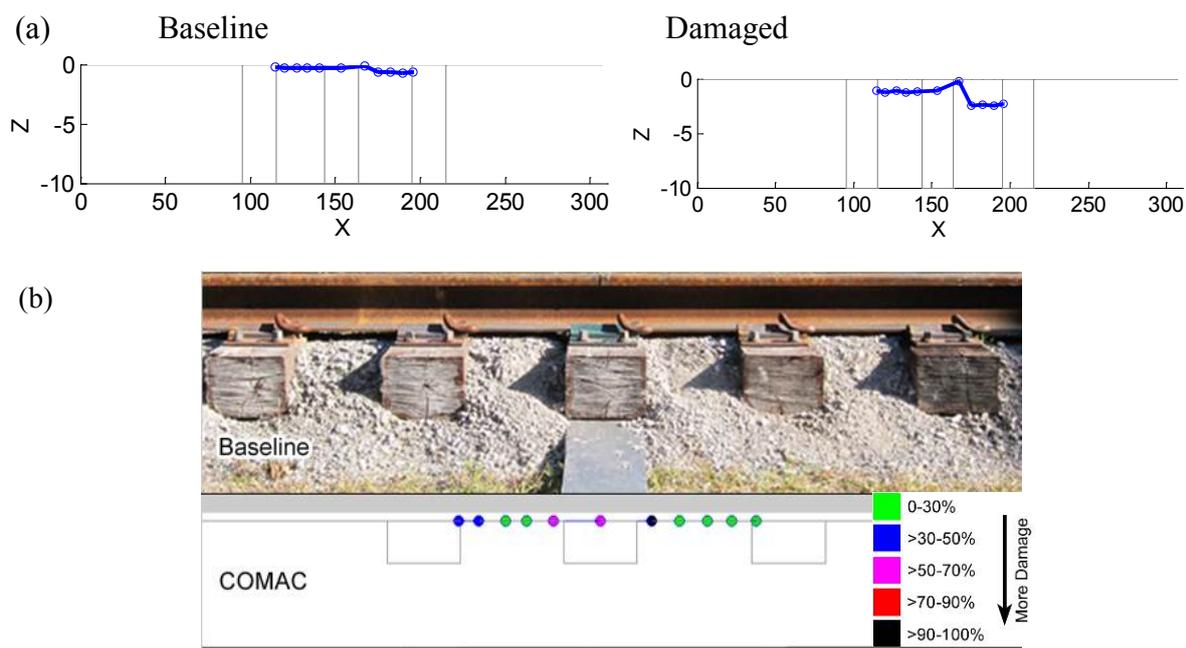
Figure 2: (a) Coordinated Mode 4 and (b) visual damage indication for one health indicator

2   SCALE BRIDGE

Based upon the general dimensions of an on-campus bridge, a 1:12 scale model reinforced concrete bridge was built by students for expanded testing. The scaled bridge consisted of two inverted T-shaped piers, two end slabs with shear keys, two end walls, and one center slab. Note that the slab thicknesses were not to scale: since a two-inch slab is impractical, a six-inch minimum slab thickness was used for enough rebar cover. The scale model bridge pieces were precast in a single concrete pour. After 35 days, the pieces were unformed and assembled inside of the lab using a forklift. One surprise was that the three cubic yards of concrete tested at an unusually high average strength of 7,110 psi (ASTM C 172 and 143). The completed product is shown in Figure 3.

Figure 3: Graduate students performing impact hammer testing on the scale model bridge

The baseline case consisted of the center slab in direct contact with the t-shaped piers directly on either side. The various damage cases were created by employing rubber bearings to simulate damage to substructural elements, such as pier columns, piles, and soil. A bottle jack on a pedestal was used to lift the center slab in order to insert and remove rubber bearings for different damage scenarios. The employed bearings varied from 1/16" to ½"-thick 40A and 70A shore durometer Buna-N rubber strips. Both asymmetric and symmetric configurations were tested.

Weighing approximately 1270 pounds, the 60"x42"x6" center slab was the target of the vibration testing. A twelve-pound PCB sledge hammer (Figure 3) impacted a wood block on the bridge, inducing multi-dimensional vibrations. A Dytran tri-axial accelerometer on a level epoxy pad measured nearly imperceptible motions, and this was repeated for 57 spatially diverse locations for each damage case. Note that two measurements were on each approach slab, which proved very helpful in separating dissimilar modes. The other 55 measurements provided a grid that will allow for mode visualization in all three directions. A National Instruments CompactDAQ recorded the accelerometer signals via NI LabVIEW, and the csv time histories were loaded into the MATLAB structural health algorithm for post-processing.

With concrete to concrete gravity connections, the "undamaged" measurements are used as a baseline for comparison. The 171 signals resulted in 31 modes less than 250 Hz. Major peaks occurred near 131 Hz and 140 Hz with five lesser peaks (near 152, 178, 201, 212, and 230 Hz). The associated mode shapes included translation, bending, torsion, and coupled combinations of these. Low frequency rigid body translation modes and their directions were used to identify potential sway weaknesses; the strongest axis was the x-direction, which indicated good confinement in the longitudinal direction. Although the joint connections were strictly concrete, as-built imperfections in boundary conditions caused mode coupling. Additionally, slab distortion modes were identified from 15 to 28 Hz. These local modes would not alter with damage and thus are excluded. A complete record of the baseline is essential to quantification of later damage.

Damage was then induced by a 1/16" 70A rubber inserted at the right pier. Within the same upper limit of 250 Hz, twenty-six modes were identified for the damaged case. The mode shapes were calculated and compared to the baseline: while similarity proved somewhat subjective, the 1/16" 70A rubber caused natural frequencies to decrease with damage as provided in Table 1. The fundamental coordinated mode was a rigid body translation in the y-direction, indicating that the most likely motion for this slab was sidesway: this is a common failure mode for bridges, so piers are often simulated via a push-over analysis. The damaged case shows similar sidesway behavior to the baseline. All other coordinated modes were coupled in nature; Mode 3 specifically demonstrated more translation with disorganized bending at the right pier where the rubber was placed.

Table 1. Resulting coordinated modes.

Coordinated Mode Number	Baseline Frequency (Hz)	Damaged Frequency (Hz)	Modal Description
1	12.23	9.53	Translation
2	64.17	51.40	Rotation & Translation
3	114.63	99.71	Torsion & Bending
4	153.83	118.10	Bending & Translation
5	224.41	216.99	Rotation & Bending

In order to quantitatively compare these modes, multiple structural health metrics were employed. The developed program has twelve different algorithms based upon seven indices, but not all are applicable to every data set. Results must be abridged herein. Modal Assurance Criteria (MAC) identified that the rubber greatly affected rigid body rotation in Modes 2 and 5. Results were

inconsistent in the y-direction. Coordinate Modal Assurance Criterion (COMAC) results showed a great sensitivity to damage, but the thresholds need more study to prevent false positives.

Since the actual stiffness matrix is unknown, a proportional flexibility matrix was found for both the damaged and undamaged cases. This was then used in three possible damage indicators: Absolute Difference, Percent Difference, and Normalized Modal Flexibility Index (ZMFI). For the scale model bridge, the absolute difference method on modal flexibility resulted in extremely small values with no trend behavior. The percent difference method resulted in extremely large values and potentially many false positives. As shown in Figure 4, ZMFI showed more accuracy and less sensitivity without false positives. Although the thresholds have been selected arbitrarily, green represents little indicated damage at that point (potentially "safe") while red and black represent much indicated damage at that point (potentially "unsafe"). A concentration of damage occurs on the right side in the y-direction: this is a good result for this case, and it shows that the sway has been released by the inserted rubber.
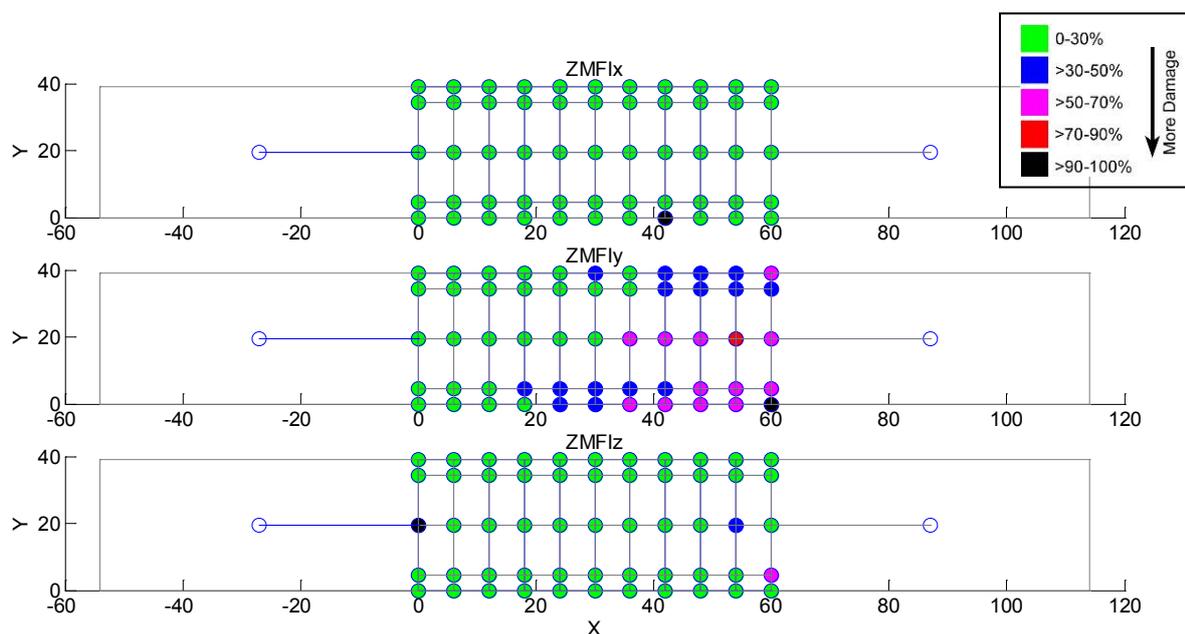

Figure 4: Normalized Modal Flexibility Index (ZMFI) results for each direction by location

Curvature estimates provide more sensitive metrics than direct mode shape comparisons. Calculated by the second derivative of the modal displacement, the curvature is calculated for both damaged and undamaged modes and then can be used in four possible damage indicators: Absolute Difference, Division, Total Division, and COMAC. The absolute difference method on curvature showed strange results: no damage in the x-direction, intermediate damage in the y-direction, and complete damage in the z-direction. Division and total division of curvatures also did not result in any discernible trends. However, performing COMAC on the curvature did indicate right side damage in the z-direction.

Calculation of the Damage Location Vector (DLV) involves direct comparison of two frequency response functions: a major advantage, no modal decomposition is required. The DLV is found by subtracting the undamaged frequency response magnitude from the damaged frequency response magnitude, and summing across all modes to quantify the fluctuations in the frequency response functions. The DLV was consistent with ZMFI in the y-direction. The outer sensor lines showed damage in the x-direction, perhaps indicating an increase in torsion. The z-direction had some outer sensor line sensitivity and both end conditions showed some level of damage.

3   FIELD BRIDGE

On the University of Mississippi campus, the Eastgate Bridge is located on University Avenue across from the Gertrude C. Ford Center and is a heavily used central connector near the famous Circle and Grove. According to drawings, the bridge was designed in 1939 by the now Mississippi Department of Transportation as a Federal State-Aid project. Its current owner and maintenance are in question, however.

Originally a highway overpass with a railroad underneath, the bridge itself is 34 feet tall with 32.6 feet clear underneath. The bridge consists of reinforced concrete decking supported by steel girders, which are then in turn supported by reinforced concrete multi-column piers. The girders are approximately 36 inches deep and 150 pounds per foot. The bridge now supports four lanes of traffic as well as two pedestrian sidewalks and major campus utilities. The bridge has a 39 degree right forward skew, serving as an important modal coupling mechanism. Including several expansion joints, it consists of two 50 foot outer decks as well as a 60 foot middle deck, where most of the measurements for the testing were taken.

While testing in one lane, traffic on the other three lanes provides excitation. The traffic control plan has limited lane closures to one at a time on deck, but the two-lane road underneath was shut down for safety. Cooperation was obtained from the City of Oxford and the University Physical Plant. From the ground, all structural members and joints seemed reasonable for a 70-year-old bridge. Significant corrosion and abutment washes were detected, but the overall bridge appeared in good condition. This experiment serves as a baseline for future damage indication testing.
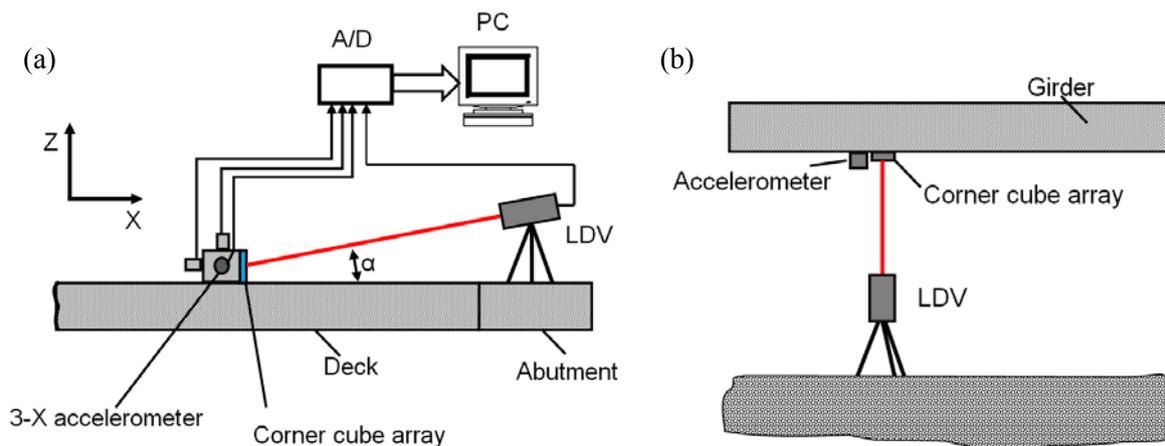

Figure 5: Measurement schematics (a) on the bridge deck and (b) underneath the bridge

Three measurement systems were employed as shown in Figure 5. A laser Doppler vibrometer (LDV) was also used on both the top and bottom of the bridge to capture surface vibration in an attempt at non-contact inspection. Measurements were taken at 36 points on the bridge deck: 28 on the center deck, 4 on the outer decks, and 4 on the abutments. Magnetic sensors as well as a prism were used for underside measurements. With the aid of a boom lift, twenty points were measured on the girders underneath the deck. A sample rate of 2000 samples per second and a sample length of 30 seconds were selected for use in the test; with publication assistance, similar tests were surveyed and preliminary frequency expectations were used for guidance. Files were saved from each run of the program as comma separated value files for later post-processing by the in-house structural health program.

Deck testing showed the uniqueness of each vehicle's time history, including even a double-decker bus. Large jumps in the amplitude were visible on each vehicle trace: these indicated

settlement on both of the bridge abutments. Sudden increases in excitation occurred due to the elevation difference at expansion joints, creating a jarring force and an audible noise when the vehicle crosses. The sensitivity of a LDV to Z- and X-components of vibration depends upon the grazing angle value α. This angle varied from 4.5 degrees for the points at the center line of the middle deck to 13 degrees for the points at the edge of outer decks. Unfortunately, these angles were too low to detect vertical motion. Possible adjustments to reduce grazing angles are needed to improve the success of remote vibration measurement of bridge decks. Alternatively, more powerful and more expensive laser instruments with larger apertures could be used.

Girder testing showed that the bottom accelerometers had connection interference, sometimes extreme, due to hanging cords. The LDV performed excellently since it had a vertical shot of approximately 30 feet. Artifacts were produced when measurements were taken without the prism. With a retroreflector, an LDV can replace accelerometers in underneath bridge vibration measurements.

CONCLUSION

These three experimental efforts work toward the same end of improved infrastructure inspection. Quantitative analysis using damage indicators showed both damage severity and location. Performance depended upon both data capture and structure type. For example, the field test showed that minimizing standoff distance and maximizing grazing angle are important. True ambient excitation may not supply enough required mode shapes to locate damage. Wind may also provide more excitation than a vehicle; however, a windy day can cause interference in the LDV signal via air turbulence.

Condition-based maintenance in real-time is a large hurdle to overcome due to the nature of decision-making on both modal coordination and corrective action. Still, the developed health evaluation program can be augmented with these capabilities after more trials. The most challenging part of the program is modal coordination, so the first developmental aspect will be additional features to make this less subjective. Research is proceeding towards finding the damage indicators that work best for different classes of structures. The health program outputs several different metrics, but which (or which combination) is preeminent for any bridge or even any structure. Safety thresholds can then be used for maintenance decision-making. After all technical challenges are resolved, a user interface must be added to the completed health program. It must be tested by state inspectors before any chance of implementation.